# ENERGY HARVESTING WIND AND HYDRO

Sheila Tobing

2025

# Outline

- Introduction
- Small-scale energy systems
- Small wind turbine (SWT) design and components
- Fundamentals of wind energy
- Wind resource assessment
- Innovative wind energy harvester
- Hydropower overview
- Classification of hydropower
- Hydraulic power
- Innovative hydro/water energy harvester
- Hybrid solar-wind power plant system

# Introduction

- Energy harvesting is a promising approach to addressing existing energy problems by extracting electricity from the environment. It involves capturing and converting energy from natural sources, such as wind and water flow, into usable electrical energy.
- Wind and hydropower are particularly attractive sources due to their abundance and potential for high power density compared to other renewable energy sources like solar energy.

# Introduction

- Wind energy harvesting utilizes wind turbines to convert the kinetic energy of wind into electricity, while hydropower energy harvesting harnesses the potential energy of water stored at a height to generate electricity through hydro turbines.
- Both wind and hydropower are considered clean energy sources as they produce minimal greenhouse gas emissions during operation, contributing to a more sustainable energy future

# Importance of small-scale energy systems

- Energy harvesting is crucial for powering small-scale, independent gadgets like wireless sensors, wearable electronics, and distant monitoring systems. These self-sufficient systems do not need batteries or external power sources, which lowers maintenance, costs, and environmental effects.
- Wind and solar energy are particularly well-suited for small-scale power generation in off-grid or isolated places where grid access is restricted or costly.
- Applications: rural electrification, microgrids, remote sensing

# Calculation of Wind Power

- To determine the power contained in the wind moving toward a WT, consider the kinetic energy, KE, of a mass of air, *m* (in kg), moving at speed, *U* (in m/s):

$$KE = \frac{1}{2} m U^2$$

- A horizontal cylinder of air of area *A* (in $m^2$) and velocity *U*, moving toward a WT.
- The area, *A*, corresponds to the area swept out by the rotating WT blades.

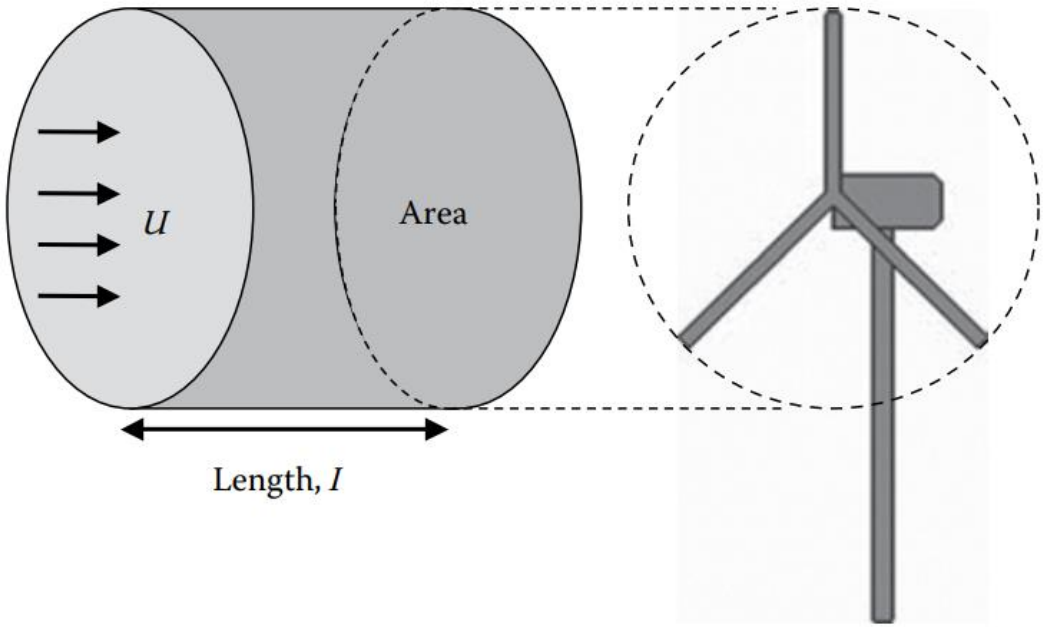

# Calculation of Wind Power

- The mass $m$ of the air column is volume $V$ times the density, where $\rho$ represents the air density in kg/

$\rho$ is the air density, kg/m$^3$
$V$ is the volume, m$^3$
$A$ is the area, m$^2$
$l$ is the length, m
$U$ is the wind speed, m/s
$t$ is the time, s

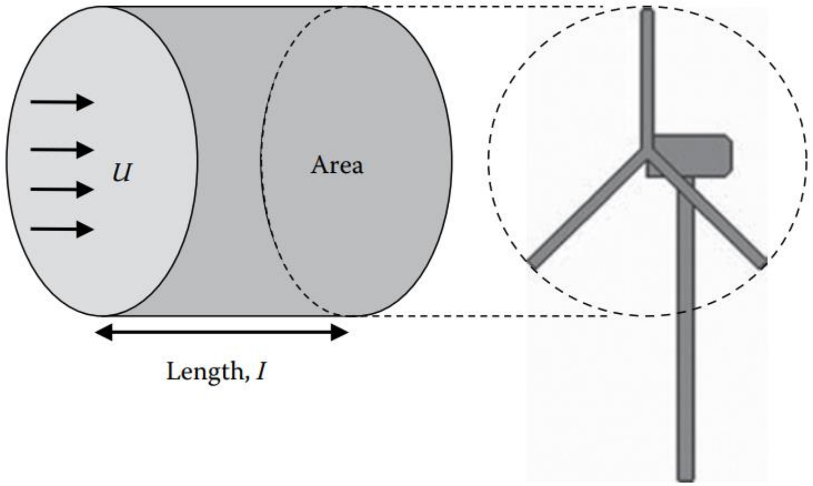


$$m = \rho V = \rho A l = \rho A U t$$

- The length of the column of air, $l$, is equal to the distance the wind travels in a given time interval, $t$, and is found by multiplying the wind speed, $U$, by the time.

# Calculation of Wind Power

$$KE = \frac{1}{2}mU^2 = \frac{1}{2}(\rho AUt)U^2 = \frac{1}{2}\rho AtU^3$$

- Dividing the KE by time yields the power of a moving column of air:

$$\text{Power} = \frac{KE}{t} = \frac{1}{2}\rho AU^3$$

- The power in a column of wind is linearly proportional to the air density and area of the air column.
- The power is also proportional to the cube of the wind speed.

# Calculation of Wind Power

- The circular area swept out by the turbine blades is proportional to the blade radius squared (*$R^2$*), turbine power is also proportional to the blade radius squared (*$R^2$*):

$$\text{Power} = \frac{1}{2}\rho A U^3 = \frac{1}{2}\rho \pi R^2 U^3$$

- Longer blade lengths and taller turbines (providing access to higher wind speeds) are options to increasing WT power output.
- Longer blades need more sophisticated manufacturing techniques to build blades strong enough to withstand wind gusts and extreme wind speeds (in excess of 100 mph).
- Taller towers must be strong enough to withstand the forces transmitted from the blades, weight of the nacelle, and other parts while still being cost-effective.
- Transporting turbine blades from manufacturing facilities to installation sites also becomes more challenging and more costly.

# Coefficient of Performance

- The coefficient of performance, $C_P$, which is a ratio of the aerodynamic power extracted by the WT, $P_{aero}$, divided by the total power in the wind, $P_{wind}$, and is calculated as:

$$C_p = \frac{P_{aero}}{P_{wind}} = \frac{P_{aero}}{1/2\,\rho A U^3} = \frac{P_{aero}}{1/2\,\rho \pi R^2 U^3}$$

→ pakai U relatif

- The theoretical maximum turbine efficiency was derived by Albert Betz in 1920 and is:

$$C_p = \frac{16}{27} \approx 0.59 = \text{Betz limit}$$

→ horizontal axis only

# Maximum wind-turbine efficiency: The Betz limit

Source: Mathew, Sathyajith. Wind energy: fundamentals, resource analysis and economics. Vol. 1. Berlin: Springer, 2006.

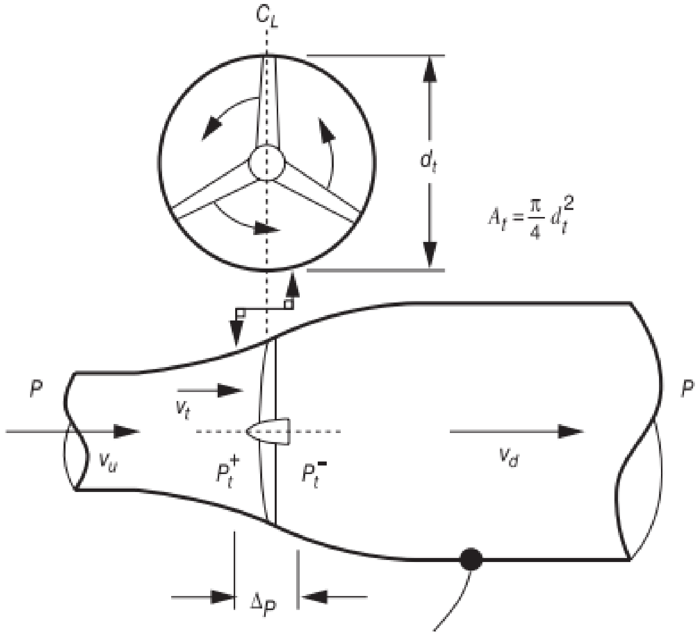


- It is common practice to estimate maximum attainable efficiency for a wind turbine using an ideal, somewhat oversimplified, fluid flow mode

- The force on the disc (turbine blades) is the area times the rate of change of momentum between the upstream and downstream fluid, while the power extracted is force times velocity; hence:

$$F = \rho A v_t (v_u - v_d),$$

$$P = \rho A v_t^2 (v_u - v_d).$$

# Maximum wind-turbine efficiency: The Betz limit

Source: Mathew, Sathyajith. Wind energy: fundamentals, resource analysis and economics. Vol. 1. Berlin: Springer, 2006.

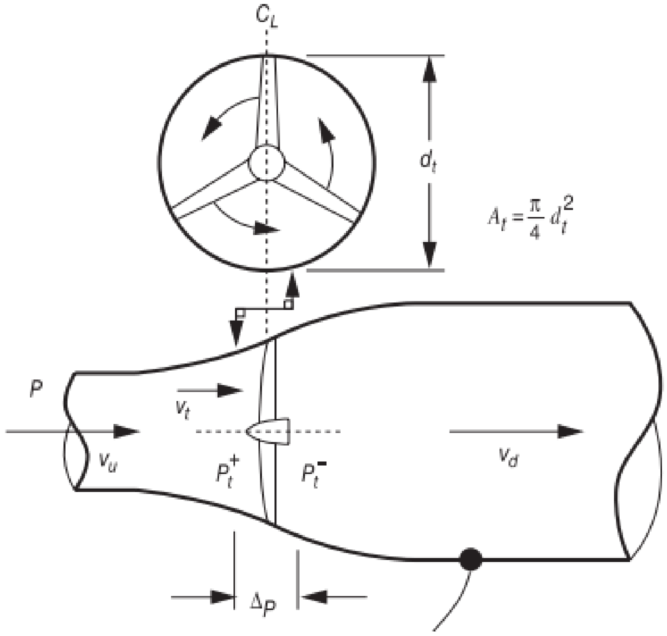


- Now we apply the Bernoulli relation

Upstream: $$p_t^+ + \frac{1}{2}\rho v_t^2 = p + \frac{1}{2}\rho v_u^2 ,$$

Downstream: $$p_t^- + \frac{1}{2}\rho v_t^2 = p + \frac{1}{2}\rho v_d^2 ,$$

- The total force is:

$$F = A_t \Delta p = A_t \left(p_t^+ - p_t^-\right) = \frac{A_t}{2}\rho\left(v_u^2 - v_d^2\right),$$

$$F = \rho A_t \left(v_u - v_d\right)\left(\frac{v_u + v_d}{2}\right).$$

# Maximum wind-turbine efficiency: The Betz limit

Source: Mathew, Sathyajith. Wind energy: fundamentals, resource analysis and economics. Vol. 1. Berlin: Springer, 2006.

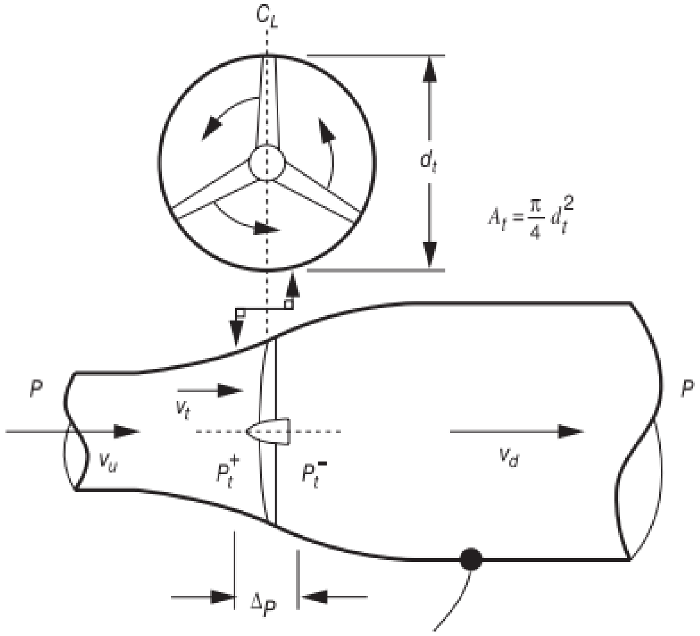


- Comparing the first and last equations for F , we see that

$$v_t = \left(\frac{v_u + v_d}{2}\right).$$

$$(v_u - v_d) = 2(v_u - v_t),$$

- So, the power $P = 2\rho A_t v_t^2 (v_u - v_t).$
- Divide the power with upstream airflow $(\rho A_t v_u^3/2)$ gives the **power coefficient**

$$\eta = 4\left(\frac{v_t}{v_u}\right)^2 \left[1 - \left(\frac{v_t}{v_u}\right)\right].$$

- Set $\partial\eta / \partial v_t = 0$ and we get

$$\eta_{max} = 4\left(\frac{2}{3}\right)^2 \left[1 - \left(\frac{2}{3}\right)\right] = \frac{16}{27} = 0.593,$$

# Small wind turbine (SWT) design and components

- Wind turbines are categorized as small when they generate less than 100 kilowatts (kW) of electricity, and they are frequently employed in residential, commercial, and agricultural settings ( Mathew, 2006).
- Small wind turbines typically consist of a rotor with two or three blades, a nacelle housing the generator and gearbox, and a tower to elevate the turbine (Manwell et al., 2009). However, there are small wind turbines with more than three blades. SWT with more blades or higher solidity is usually implemented in low wind speed regions because they can generate high torque in low wind speed compared to the conventional two- or three-blade horizontal axis wind turbine.

# Wind Variability

- The wind's variability can be characterized by a number of statistical properties:

  - Turbulence intensity
  - Turbulent kinetic energy
  - Autocorrelation
  - Integral time scale/length scale
  - Power spectral density function

# Turbulence Intensity

→ informing how turbulent the area is

- Turbulence intensity: the ratio of the standard deviation of the wind speed to the mean wind speed.
- The sample rate is normally at least once per second (1 Hz).
- Turbulence intensity (TI) is frequently in the range of 0.1 to 0.4
- The highest TI occur at the lowest wind speeds.

$$TI = \frac{\sigma_u}{U} \qquad \sigma_u = \sqrt{\frac{1}{N_s - 1}\sum_{i=1}^{N_s}(u_i - U)^2}$$

- Ns = number of samples during each short-term interval
- Ui = wind speed for a sequence of samples
- U = mean wind speed
- σu = Standard Deviation

# Wind Variability

- Turbulent kinetic energy

  TKE represents the energy associated with turbulent motion in the wind flow. It is calculated as the sum of the kinetic energy of turbulent fluctuations in wind speed, direction, and other parameters. TKE is essential for understanding the intensity and scale of turbulence within a wind resource area.

average of fluctuation, squared.

$$TKE = \frac{1}{2}\left(\overline{u'^2} + \overline{v'^2} + \overline{w'^2}\right)$$

Where:

- $TKE$ is the turbulent kinetic energy,
- $u'$, $v'$, and $w'$ are the turbulent velocity fluctuations in the $x$, $y$, and $z$ directions, respectively, and
- The overbar represents a time or spatial average.

# Wind Speed PDF, Autocorrelation, Integral Time Scale

- Autocorrelation

The autocorrelation function of wind speed is a statistical measure that quantifies the degree of correlation between wind speed values at different points in time. It is a fundamental tool used in analyzing the temporal correlation structure of wind speed data.

Mathematically, the autocorrelation function $R(\tau)$ of wind speed is defined as:

$$R(\tau) = \frac{\langle (v(t)-\mu_v)(v(t+\tau)-\mu_v) \rangle}{\sigma_v^2}$$

Where:

- $\tau$ is the time lag or the interval between two wind speed measurements,
- $v(t)$ is the wind speed at time $t$,
- $\mu_v$ is the mean wind speed,
- $\langle \cdot \rangle$ denotes the average over the time series, and
- $\sigma_v^2$ is the variance of the wind speed.

# Wind Speed PDF, Autocorrelation, Integral Time Scale

- Integral time scale

In turbulence flow, the integral time scale (or integral scale) represents the characteristic time over which turbulent eddies of different sizes contribute significantly to the overall turbulent motion. It is a measure of the temporal extent of turbulent structures in the flow.

For a stationary and homogeneous turbulent flow, the integral time scale *T* can be defined as:

$$T = \int_0^\infty R(\tau) d\tau$$

→ integral of autocorrelation

besar → slow changing
kecil → fast ''

Where:

- $R(\tau)$ is the autocorrelation function of the flow variable (e.g., velocity),
- $\tau$ is the time lag or interval between two measurements,
- The integral is taken over all time lags from 0 to infinity.

# Wind Speed PDF, Autocorrelation, Integral Time Scale

- Integral time scale

In atmospheric science and wind energy, for example, the integral time scale is essential for understanding the temporal variability of wind speed and turbulence in the atmospheric boundary layer.

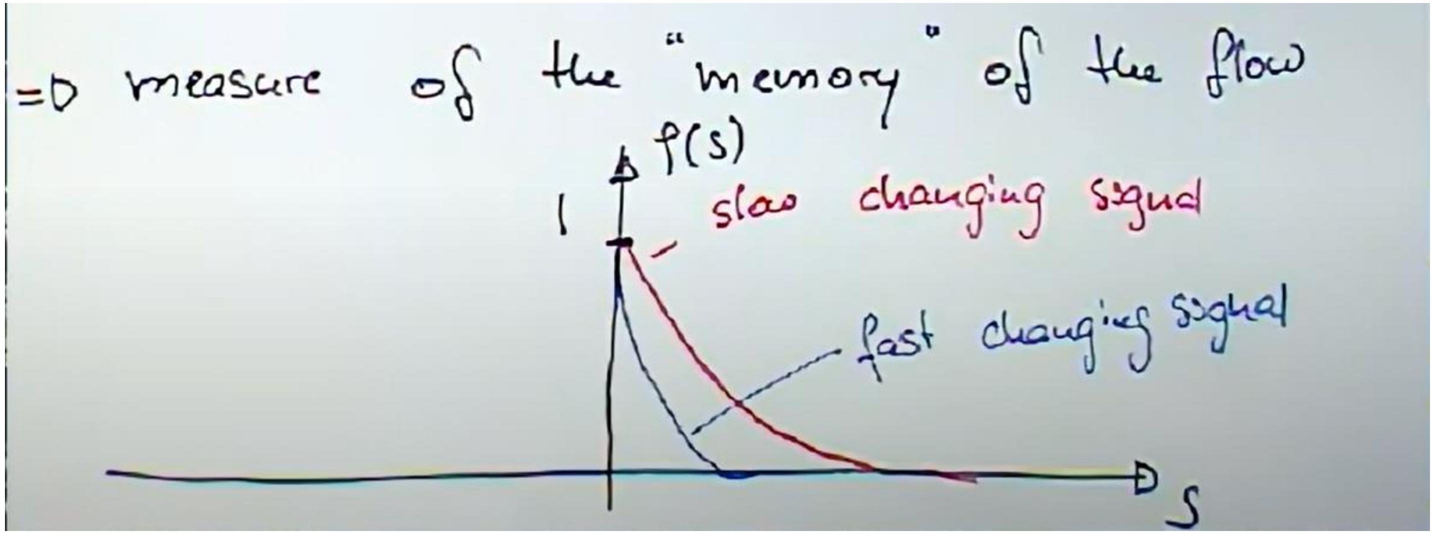


https://www.youtube.com/watch?v=wIhsXOyhNZU

# Wind Speed PDF, Autocorrelation, Integral Time Scale

- Integral time scale
  - The integral time scale cannot be negative because the autocorrelation function is always non-negative.
  - The integral time scale measures how wind speed at one time correlates with wind speed at a later time.
  - The typical range of the integral time scale is **1 to 100 seconds**, depending on factors such as height, terrain, and atmospheric stability.
  - The integral time scale is used to model wind turbulence and assess the fatigue loads on wind turbine components. A larger integral time scale indicates more persistent wind speed fluctuations, which can affect the design and operation of wind turbines.

# Power Spectral Density Function

- Power spectral density (PSD): the function describing the relation between frequency and amplitudes of sinusoidally varying waves making up the fluctuating wind speed.
- The average power in the turbulence over a range of frequencies may be found by integrating the PSD between two frequencies.
- The integral over all frequencies is equal to the total variance.
- PSD are often used in dynamic analyses.
- A number of PSD functions are used as models in wind energy engineering when representative turbulence PSD are unavailable for a given site. A suitable model that is similar to the one developed by von Karman for turbulence in wind tunnels.

$$S(f) = \frac{\sigma_u^2 4(L/U)}{\left[1 + 70.8(f\,L/U)^2\right]^{5/6}}$$

f : frequency (Hz)
L: the integral length scale
U: the mean wind speed at the height of interest

# Aeroelastic Piezoelectric Energy Harvesters
# Small-Scale Windmill and Wind Turbine.

- Previous research indicates that the main obstacle of small electromagnetic wind mills is the much lower power generating efficiency in slow flows.
- The output power can be significantly raised if a more advanced small-scale wind turbine can be built using optimal shape of airfoil and appropriate diffuser design.
- Piezoelectric transduction small-scale windmills have lately shown great promise in effectively collecting low speed flow energy. The oscillatory motion of the piezoelectric transducer is transferred from the rotation of the windmill shaft under wind flows. With a working concept similar to that of a mechanical stopper, the mechanical transfer is occasionally achieved by direct impact between the piezoelectric cantilever and the cam or blade; some other times it is achieved by magnetic interfaction (dipolar force between colloidal particles), where no contact impact is necessary.

Liya Zhao and Yaowen Yang. Toward Small-Scale Wind Energy Harvesting: Design, Enhancement, Performance Comparison, and Applicability. Shock and Vibration Volume 2017, Article ID 3585972, 31 pages, https://doi.org/10.1155/2017/3585972.

# Aeroelastic Piezoelectric Energy Harvesters - Small-Scale Windmill and Wind Turbine.

Table 1: Summary of various small-scale windmills and wind turbines.

| Transduction | Mechanical transfer | Cut-in wind speed (m/s) | Cut-out wind speed (m/s) | Maximum power (mW) | Wind speed at max power (m/s) | Dimensions | Power density per swept area ($mW/cm^2$) | Advantages/disadvantages |
|---|---|---|---|---|---|---|---|---|
| Electromagnetic | — | — | — | 130 | 11.8 | 4.2 cm in dia. | 9.38 | (i) High power generation efficiency at high wind speed.<br>(ii) At low wind speed, efficiency decreased sharply due to the friction in the generator and the internal electric resistance |
| Electromagnetic | — | 3 | — | 4.3 | 10 | 3.2 cm in dia. | 0.535 | (i) Bearing loss and resistive generator loss limits the miniaturization of the turbine |
| Piezoelectric | Contact via mechanical stopper | — | — | 10.2 | — | 12 bimorphs in a circular array, each of $6 \times 2 \times 0.05$ $cm^3$ | 0.0902 | (i) Proves the feasibility of efficiently harvesting low speed wind energy using piezoelectric materials.<br>(ii) Bimorphs are not vibrating in phase so the output has to be individually processed |
| Piezoelectric | Contact via mechanical stopper | 2.1 | 5.4 | 7.5 | 4.5 | 10 bimorphs in a circular array, each of $6 \times 2 \times 0.06$ $cm^3$ | 0.0663 | |
| Piezoelectric | Contact via mechanical stopper | 2.1 | 6.2 | 1.2 | 5.4 | $5.08 \times 11.6 \times 7.62$ $cm^3$ | 0.0134 | (i) Easy to fabricate.<br>(ii) Space efficient with a rectangular-array arrangement of transducers.<br>(iii) Combined circuit can be used because all the bimorphs are vibrating in phase.<br>(iv) Power was much lower compared to the circular windmill |
| Piezoelectric | Contact via mechanical stopper | 2.4 | — | 5 | 4.5 | $7.62 \times 10.16 \times 12.70$ $cm^3$ | 0.0388 | (i) Captured wind energy is increased by employing three fan blades |
| Piezoelectric | Contact-less via magnetic interaction | 0.9 | — | 1.2 | 4.0 | $16.51 \times 16.51 \times 22.86$ $cm^3$; | $3.18 \times 10^{-3}$ | (i) Minimizing the frictional loss by avoiding direct mechanical contact.<br>(ii) Prolonging the fatigue life of piezoelectric elements.<br>(iii) Lowering down the cut-in wind speed |
| Piezoelectric | Contact-less via magnetic interaction | 2 | — | 4 | 10 | $8 \times 8 \times 17.5$ $cm^3$ | 0.0286 | (i) Introducing nonlinearity into the harvester.<br>(ii) Utilizing both nonlinear parametric excitation and ordinary excitation and helping to achieve low cut-in wind speed, high output power, and large operational range of wind speed |

Liya Zhao and Yaowen Yang. Toward Small-Scale Wind Energy Harvesting: Design, Enhancement, Performance Comparison, and Applicability. Shock and Vibration Volume 2017, Article ID 3585972, 31 pages, https://doi.org/10.1155/2017/3585972.

# Energy Harvesters Based on Vortex-Induced Vibrations

**Concept**

- Wind flow around a structure creates oscillating vortices. This oscillating movement can be converted to electricity. Wind energy is converted into electricity using piezoelectric materials.

**Examples**

- Vortex Bladeless Wind Energy System.

**Advantages**

- No moving parts (low maintenance), reduced wear and tear, lower maintenance.
- Works at low wind speeds

**Disadvantages**

- Lower efficiency compared to traditional turbines

Liya Zhao and Yaowen Yang. Toward Small-Scale Wind Energy Harvesting: Design, Enhancement, Performance Comparison, and Applicability. Shock and Vibration Volume 2017, Article ID 3585972, 31 pages, https://doi.org/10.1155/2017/3585972.

# Energy Harvesters Based on Vortex-Induced Vibrations

| Author | Transduction | Bluff body shape | Cut-in wind speed (m/s) | Cut-out wind speed (m/s) | Maximum power (mW) | Wind speed at max power (lock-in) (m/s) | Dimensions | Power density per volume ($mW/cm^3$)*1 | Advantages/disadvantages and other information |
|---|---|---|---|---|---|---|---|---|---|
| Allen and Smits [42] (in water) | Piezoelectric | Plate | 0.05 (water speed) | 0.8 (water speed) | — | — | Bluff body, frontal dimension: 5.05 cm & 3.81 cm. Eel membrane, length: 45.7 cm & 7.6 cm | | (i) Investigated and confirmed the feasibility of harvesting fluid energy via VIV. (ii) Determines that optimal performance occurs at resonance condition |
| Taylor et al. [43] (in water) | Piezoelectric | Plate | — | — | 3 V (peak voltage) | 0.5 (water speed) | PVDF eel: 24 cm × 7.6 cm × 150 $\mu$m | 1.10 ($V/cm^3$) | |
| Robbins et al. [44] | Piezoelectric | Cylinder | — | — | 7.8 | 6.7 | Flapping PVDF membrane: 25.4 cm × 17.78 cm × 457.2 $\mu$m | 0.378 | (i) The use of windward bluff body and mass on the free end of the flapping piezoelement can enhance energy conversion. (ii) Experimentally proves the use of quasi-resonant rectifier can increase the efficiency by a factor of 2.3 compared to a standard full-wave rectifier. (iii) Theoretically confirms the use of AFC/MFC can increase the efficiency by a factor of 25 compared to PVDF |
| Pobering and Schwesinger [45] | Piezoelectric | Polygon | 4.5 | 45 | 0.108 | 45 | Bluff body frontal dimension: 1.035 cm. Three identical cantilevers: 1.4 × 1.18 × 0.035 $cm^3$ | 0.0817 | (i) The use of piezoelectric bimorph cantilever ensures only the first mode deformation to guarantee no charge cancellation on the surface. (ii) Theoretically proposes the optimal geometry of $L/D = 2.125$. (iii) Adjacent cantilevers arrangement enhances output power |
| Pobering et al. [46] | Piezoelectric | D-shape | 15 | — | 1 | 40 | Bluff body frontal dimension: 1.035 cm. Nine identical cantilevers (Series 1): 2.2 × 1.18 × 0.035 $cm^3$ | 0.164 | (i) Experimentally validates the optimal geometry of $L/D = 2.125$. (ii) Use of stapled piezoelectric layers enhance output power. (iii) Adjacent cantilevers arrangement can further lower the cut-in wind speed down to 8 m/s |
| Akaydin et al. [47]; Akaydın et al. [48] | Piezoelectric | Cylinder | — | — | 0.004 | 7.23 | Bluff body: 3 cm in dia., 1.2 m in length. Cantilever: 3 × 1.6 × 0.02 $cm^3$ | $4.72 \times 10^{-6}$ | (i) The driving mechanism of the beam's oscillation was discovered via CFD as the combined effect of the overpressure resulting from the stagnation region and the suction of the core of another vortex on the opposite side. (ii) The optimal position of the upstream tip of the cantilever was found to along the centerline and at a distance of $x/D = 2$. (iii) Nonattachment of bluff body and cantilever results in very low output power |

Liya Zhao and Yaowen Yang. Toward Small-Scale Wind Energy Harvesting: Design, Enhancement, Performance Comparison, and Applicability. Shock and Vibration Volume 2017, Article ID 3585972, 31 pages, https://doi.org/10.1155/2017/3585972.

# Energy Harvesters Based on Vortex-Induced Vibrations

Table 2: Continued.

| Author | Transduction | Bluff body shape | Cut-in wind speed (m/s) | Cut-out wind speed (m/s) | Maximum power (mW) | Wind speed at max power (lock-in) (m/s) | Dimensions | Power density per volume ($mW/cm^3$)*[1] | Advantages/disadvantages and other information |
|---|---|---|---|---|---|---|---|---|---|
| Akaydin et al. [23] | Piezoelectric | Cylinder | — | — | 0.1 | 1.192 | Bluff body: 1.98 cm in dia., 20.3 cm in length. Cantilever: 26.7 × 3.25 × 0.0635 $cm^3$ | $1.47 \times 10^{-3}$ | (i) Attachment of the cylinder on the cantilever tip and use of PZT instead of PVDF greatly enhanced the output power. (ii) Attachment of the cylinder on the cantilever tip reduces the resonance wind speed for maximum power |
| Weinstein et al. [49] | Piezoelectric | Cylinder | 2 | 5 (5.5) | 5 | 5.5 | Bluff body: 2.5 cm in dia., 11 cm in length. Cantilever: 2.86 × 0.63 × 0.25 $cm^3$. Whole plane size: 22.5 × 11 $cm^2$ | 0.0918 | (i) Operational wind speed range is broadened, because the harvester's resonance frequency and its resonance wind speed can be tuned by adjusting the position of the added weight. (ii) Tuning mechanism is not automatic |
| Gao et al. [50] | Piezoelectric | Cylinder | 3.1 | — | 0.03 | 5 (turbulent flow speed) | Bluff body: 2.91 cm in dia., 3.6 cm in length. Cantilever: 3.1 × 1.0 × 0.0202 $cm^3$ | $1.25 \times 10^{-3}$ | (i) Turbulent flow results in higher output power of harvester than laminar flow. (ii) Turbulence excitation is claimed to be the dominant driving mechanism of the harvester; vortex shedding excitation in the lock-in region gives add-on contribution. (iii) Cantilever and cylinder are in parallel |
| Wang and Ko [51] | Piezoelectric | N.A. | — | — | $2 \times 10^{-4}$ | — | PVDF film: 2.5 × 1.3 × 0.0205 $cm^3$ | $3.00 \times 10^{-3}$ | |
| Wang et al. [52] | Electromagnetic | Trapezoidal | — | — | $1.77 \times 10^{-3}$ | 1.38 (water speed) | Bluff body: 4.25 mm & 1 mm in bases, 1.63 mm in height. Magnet: 0.8 × 0.8 × 1 $cm^3$ Coil: 2 cm in dia., 0.2 cm in thickness | $1.33 \times 10^{-3}$ | (i) Can be easily deployed in the pipelines, tire cavities, or machinery by installing a diaphragm on the wall. (ii) Output power is relatively low compared to other devices. (iii) Methods of enhancing power are proposed, for example, optimizing the blockage ratio, adjusting the diaphragm position, and using material with high piezoelectric constants |
| Tam Nguyen et al. [53] | Piezoelectric | Triangle | — | — | $5.9 \times 10^{-7}$ | 20.7 | Two identical bluff bodies: 0.425 cm in base length, 0.218 cm in altitude. PVDF film: 2.5 × 1.3 × 0.0205 $cm^3$ | $3.70 \times 10^{-6}$ | |

[1] If more than one sized prototypes were investigated in the reference, the information of dimension and critical wind speeds listed in the table corresponds to the one giving maximum output power.
*[1] The device volume is approximated without considering the piezoelectric element volume, thus the power density calculated is the conservative estimates showing the upper bound.

Liya Zhao and Yaowen Yang. Toward Small-Scale Wind Energy Harvesting: Design, Enhancement, Performance Comparison, and Applicability. Shock and Vibration Volume 2017, Article ID 3585972, 31 pages, https://doi.org/10.1155/2017/3585972.

# Energy Harvesters Based on Galloping

**Concept**

- Galloping is an aeroelastic instability where the structure oscillates at a low frequency due to aerodynamic forces.
- The difference between galloping and vortex-induced vibration is the cause of excitation. VIV is caused by vortex shedding, while galloping is due to the shape of the structure.
- Aerodynamic instability leads to self-excited oscillations in flexible structures. This oscillating movement can be converted to electricity.
- It is not until recently that the aeroelastic instability phenomenon of transverse galloping is employed to obtain structural vibrations for energy harvesting purposes. Due to the self-excited and self-limiting characteristics of galloping, it is a prospective energy source for energy harvesting. Moreover, compared to the VIV, galloping has its advantages of large oscillation amplitude and the ability to oscillate in an infinite range of wind speeds.

Liya Zhao and Yaowen Yang. Toward Small-Scale Wind Energy Harvesting: Design, Enhancement, Performance Comparison, and Applicability. Shock and Vibration Volume 2017, Article ID 3585972, 31 pages, https://doi.org/10.1155/2017/3585972.

# Energy Harvesters Based on Galloping

**Designs**

- Cantilever beam with a bluff body.
- Piezoelectric materials convert mechanical strain into electricity. Piezoelectric materials are distinctive materials that produce electrical charge when subjected to mechanical stress. Examples of commercial piezoelectric materials are lead zirconate titanate, barium titanate, and quartz.

**Advantages**

- Effective in low-speed wind environments.
- Simple mechanical design, easy to implement and maintain.

**Disadvantages**

- Efficiency depends on the aeroelastic properties of the structure.
- Galloping is only effective over a narrow range of wind speeds, and the placement of the harvester can be difficult.

Liya Zhao and Yaowen Yang. Toward Small-Scale Wind Energy Harvesting: Design, Enhancement, Performance Comparison, and Applicability. Shock and Vibration Volume 2017, Article ID 3585972, 31 pages, https://doi.org/10.1155/2017/3585972.

# Energy Harvesters Based on Wake Galloping

- The galloping piezoelectric energy harvester can be classified into two types of galloping mechanisms: transverse galloping and wake galloping.
- The transverse galloping based PEH contains a prismatic construction (square, D-shape, or triangle, etc.) and piezoelectric materials which are attached to the free and fixed ends of elastic cantilever beam. When, the flow velocity exceeds a critical value, the bluff body subjected into the airflow, is affected by transverse fluctuations, called galloping.

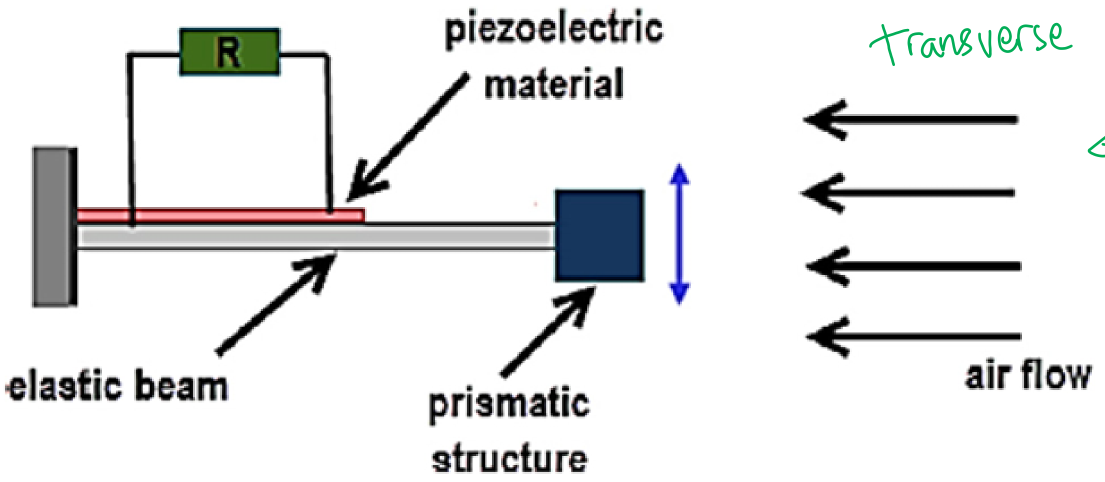


transverse galloping

air flow //
long structure

# Energy Harvesters Based on Galloping

| Author | Transduction | Bluff body shape | Cut-in wind speed (m/s) | Cut-out wind speed (m/s) | Maximum power (mW) | Wind speed at max power (m/s) | Dimensions | Power density per volume (mW/cm$^3$) | Advantages/disadvantages and other information |
|---|---|---|---|---|---|---|---|---|---|
| Sirohi and Mahadik [54] | Piezoelectric | Triangle | 3.6 | 6.1 | 50 | 5.2 | Bluff body: 4 cm in side, 25.1 cm in length; cantilever: 16.1 × 3.8 × 0.0635 cm$^3$ | 0.281 | (i) High peak power is achieved, with high electromechanical coupling. (ii) Validates the feasibility of predicting galloping energy harvester's response with quasi-steady hypothesis. (iii) Abrupt decrease in output power at 6.1 m/s is undesired. |
| Sirohi and Mahadik [55] | Piezoelectric | D-shape | 2.5 | — | 1.14 | 4.7 | Bluff body: 3 cm in dia., 23.5 cm in length; cantilever: 9 × 3.8 × 0.0635 cm$^3$ | 0.0134 | (i) Output power continuously increases with wind speed, with no cut-out wind speed. (ii) Wide operational wind speed range. (iii) Requiring turbulent flow to function well, for example, flow from a rotating fan, because D-shape cannot self-oscillate in laminar flow. (iv) Cantilever and bluff body prism are in parallel. |
| Zhao et al. [56]; Yang et al. [32] | Piezoelectric | Square | 2.5 | — | 8.4 | 8.0 | Bluff body: 4 × 4 × 15 cm$^3$; cantilever: 15 × 3 × 0.06 cm$^3$ | 0.0346 | (i) Experimentally determining for the first time that the square section is optimal for galloping energy harvesting compared to other shapes, giving the largest power and the lowest cut-in wind speed. (ii) High peak power is achieved, with high electromechanical coupling. (iii) Wide operational wind speed range. |
| Zhao et al. [57] | Piezoelectric | Square | 1.0 | — | 4 | 5.0 | Bluff body: 4 × 4 × 15 cm$^3$; cut-out cantilever: inner beam: 5.7 × 3 × 0.03 cm$^3$; outer beam: 17.2 × 6.6 × 0.06 cm$^3$ with cut out at the inner beam location | 0.0162 | (i) 2DOF cut-out structure with magnetic interaction. (ii) Reducing the cut-in speed. (iii) Enhancing output power in the low wind speed range. (iv) Having stiffness nonlinearity induced by magnetic interaction. (v) Output power is limited in high wind speeds. |
| Zhao and Yang [24] | Piezoelectric | Square | 2.0 | — | 12 | 8.0 | Bluff body: 4 × 4 × 15 cm$^3$; cantilever: 27 × 3.4 × 0.06 cm$^3$; beam stiffener: 8 × 4.5 × 0.5 cm$^3$ | 0.0455 | (i) Employed beam stiffener as electromechanical coupling magnifier. (ii) Effective for all three types of harvesters based on galloping, vortex-induced vibration and flutter, with greatly enhanced output power. (iii) Displacement is not increased, thus not aggravating fatigue problem. (iv) Easy to implement. (v) Cut-in wind speed is undesirably increased. |

Liya Zhao and Yaowen Yang. Toward Small-Scale Wind Energy Harvesting: Design, Enhancement, Performance Comparison, and Applicability. Shock and Vibration Volume 2017, Article ID 3585972, 31 pages, https://doi.org/10.1155/2017/3585972.

# Energy Harvesters Based on Galloping

| Author | Transduction | Bluff body shape | Cut-in wind speed (m/s) | Cut-out wind speed (m/s) | Maximum power (mW) | Wind speed at max power (m/s) | Dimensions | Power density per volume (mW/cm$^3$) | Advantages/disadvantages and other information |
|---|---|---|---|---|---|---|---|---|---|
| Zhao et al. [33, 58] | Piezoelectric | Square | 3.5 | — | 1.14 | 5.0 | Bluff body: $2 \times 2 \times 10$ cm$^3$; cantilever: $13 \times 2 \times 0.06$ cm$^3$ | 0.0274 | (i) Employed synchronous charge extraction (SCE) eliminates the requirement of impedance matching and ensures the flexibility of adjusting the harvester for practical applications. (ii) Saving 75% of piezoelectric materials by the SCE compared to the standard circuit. (iii) Achieving smaller transverse displacement and alleviating fatigue problem with SCE. |
| Zhao et al. [59, 60] | Piezoelectric | Square | 3.0 | — | 3.25 | 7.0 | Bluff body: $2 \times 2 \times 10$ cm$^3$; cantilever: $13 \times 2 \times 0.06$ cm$^3$ | 0.0782 | (i) Synchronized switching harvesting on inductor (SSHI) enhances output power compared to standard circuit. (ii) SSHI shows more significant benefits in weak-coupling systems, yet loses benefits in strong-coupling conditions. (iii) Achieving 143% power increase at 7 m/s. |
| Bibo et al. [61] | Piezoelectric | Square | ≈2.2 | — | 0.348*1 | 4.5 | Bluff body: $5.08 \times 5.08 \times 10.16$ cm$^3$; cantilever: $8.5 \times 0.7 \times 0.03$ cm$^3$ | 0.0013 | (i) Concurrent flow and base excitations enhances energy harvesting. (ii) Base excitation improves electrical output in resonance region. (iii) Electrical output drops if base excitation frequency is close to but outside of resonance region. |
| Ewere and Wang [62] | Piezoelectric | Square | 2 | — | 13 | 8 | Bluff body: $5 \times 5 \times 10$ cm$^3$; cantilever: $22.8 \times 4 \times 0.04$ cm$^3$; bump stop: gap size: 0.5 cm, contact area: $1.27 \times 4$ cm$^2$; location: 13 cm along cantilever | 0.0512 | (i) Incorporating an impact bump stop successfully relieves the fatigue problem. (ii) Achieving substantial 70% reduction in displacement amplitude with only 20% voltage reduction. |

*1 Calculated by $(5.9\ \mathrm{V})^2/100\ \mathrm{k\Omega}$ from the information given in Table 1 and Figure 12 of the reference.

Liya Zhao and Yaowen Yang. Toward Small-Scale Wind Energy Harvesting: Design, Enhancement, Performance Comparison, and Applicability. Shock and Vibration Volume 2017, Article ID 3585972, 31 pages, https://doi.org/10.1155/2017/3585972.

# Energy Harvesters Based on Flutter

→ Bentuk aerodinamis, struktur ringan

**Concept**

- Flutter is a self-excited aeroelastic instability, where the interaction of elastic structure deformation with aerodynamic forces creates periodic motion.
- Aeroelastic instability where aerodynamic forces induce vibrations.
- Utilized in airfoil-based energy harvesters. Energy is harvested from the flutter caused by the wind passing over the airfoil.

**Examples**

- Piezoelectric beams with fluttering motion.

Liya Zhao and Yaowen Yang. Toward Small-Scale Wind Energy Harvesting: Design, Enhancement, Performance Comparison, and Applicability. Shock and Vibration Volume 2017, Article ID 3585972, 31 pages, https://doi.org/10.1155/2017/3585972.

# Energy Harvesters Based on Flutter

**Advantages**

- Higher energy density compared to VIV and galloping.
- Can be integrated into aircraft wings for self-powered sensors.

**Disadvantages**

- Complex aerodynamic design, sensitive to wind conditions.

Liya Zhao and Yaowen Yang. Toward Small-Scale Wind Energy Harvesting: Design, Enhancement, Performance Comparison, and Applicability. Shock and Vibration Volume 2017, Article ID 3585972, 31 pages, https://doi.org/10.1155/2017/3585972.

# Energy Harvesters Based on Flutter vs. VIV

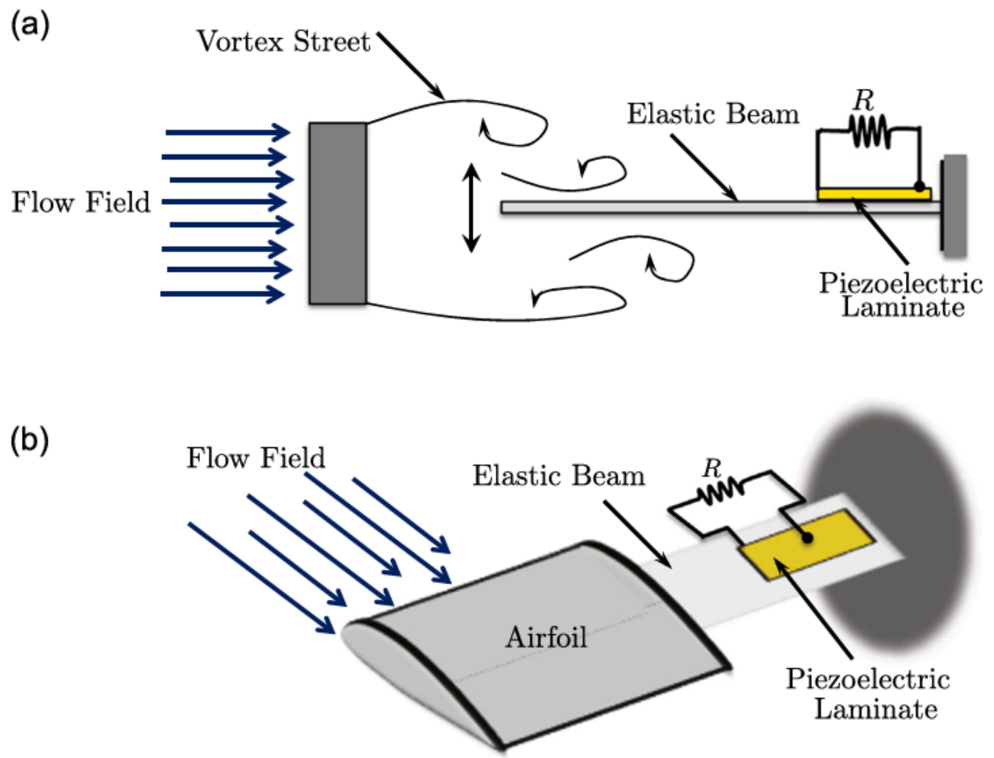


**Fig. 1.** Cartoon schematics of piezoaeroelastic energy harvester. (a) Vortex street induced oscillations and (b) flutter induced oscillations.

# Energy Harvesters Based on Flutter vs. VIV

- Piezoelectric vibratory energy harvesting: mechanical vibrations are transformed into electricity via the piezoelectric effect.
- Piezoaeroelastic energy harvesting is the use of piezoelectric to harness energy from aerodynamic forces.
- The harvester consists of a flexible structure, a beam or a plate, with piezoelectric laminates. When placed in a flow field, the piezoaeroelastic structure is excited to undergo large amplitude oscillations due to an aeroelastic instability.
- A common approach is based on placing the harvester in the wake of a bluff body such that the Kármán vortex street forces the structure to oscillate in a periodic manner. Another approach is based on designing the flexible structure with an airfoil profile such that the flutter instability is excited when the flow speed exceeds the flutter speed.

A. Bibo, M.F. Daqaq . Journal of Sound and Vibration 332 (2013) 5086–5102

# Energy Harvesters Based on Flutter

| Author | Transduction | Flutter instability | Flap at the tip | Cut-in wind speed (flutter speed) (m/s) | Cut-out wind speed (m/s) | Maximum power (mW) | Wind speed at max power (m/s) | Dimensions | Power density per volume (mW/cm$^3$) | Advantages/disadvantages and other information |
|---|---|---|---|---|---|---|---|---|---|---|
| Bryant and Garcia [63]; Bryant and Garcia [26] | Piezoelectric | Modal convergence flutter | Airfoil, profile NACA0012 | 1.86 | — | 2.2 | 7.9 | Airfoil: semichord 2.97 cm, span 13.6 cm. Cantilever: 25.4 × 2.54 × 0.0381 cm$^3$ | $7.17 \times 10^{-3}$ | (i) Semiempirical model of the nonlinear electromechanical and aerodynamic system accurately predicted electrical and mechanical response.<br>(ii) Successfully predicts the flutter boundary with one of the real parts of the first two eigenvalues turning positive and the two imaginary parts coalescing.<br>(iii) Wide operational wind speed range.<br>(iv) Subcritical Hopf bifurcation, a large initial disturbance is fundamental for system startup. |
| Bryant et al. [64] | Piezoelectric | Modal convergence flutter | Flat plate | Stiff host structure<br>17.3<br>Compliant host structure<br>15.2 | Stiff host structure<br>29<br>Compliant host structure<br>29 | Stiff host structure<br>43<br>Compliant host structure<br>35 | Stiff host structure<br>26<br>Compliant host structure<br>25 | Flat plate tip: chord 3 cm, span 6 cm, thickness 0.79 mm. Cantilever: 7.6 × 2.5 × 0.0381 cm$^3$ | Stiff host structure 20.0<br>Compliant host structure 16.3 | (i) Compared to a stiff host structure, a compliant host structure reduces the cut-in wind speed, cut-in frequency and oscillation frequency.<br>(ii) The peak power is shifted toward the lower wind speeds with the compliant host structure. |
| Bryant et al. [65] | Piezoelectric | Modal convergence flutter | Flat plate | 17.3 | 29 | 43 | 26 | Flat plate tip: chord 3 cm, span 6 cm, thickness 0.79 mm. Cantilever: 7.6 × 2.5 × 0.0381 cm$^3$ | 20.0 | (i) Confirms the feasibility of using ambient flow energy harvesting to power aerodynamic control surfaces. |
| Erturk et al. [66] | Piezoelectric | Modal convergence flutter | Airfoil | 9.30 | — | 10.7 | 9.30 | Airfoil: semichord 12.5 cm, span 50 cm. Cantilever: — | $2.27 \times 10^{-3}$ | (i) Effect of electromechanical coupling on flutter energy harvesting is analyzed.<br>(ii) Found that the optimal load gave the maximum flutter speed due to the associated maximum shunt damping effect during power extraction. |
| Sousa et al. [67] | Piezoelectric | Modal convergence flutter | Airfoil | Linear configuration<br>12.1<br>With free play nonlinearity<br>10.0 | Linear configuration<br>—<br>With free play nonlinearity<br>— | Linear configuration<br>12<br>With free play nonlinearity<br>27 | Linear configuration<br>12.1<br>With free play nonlinearity<br>10.0 | Airfoil: semichord 12.5 cm, span 50 cm. Cantilever: — | Linear configuration $2.55 \times 10^{-3}$<br>With free play nonlinearity $5.73 \times 10^{-3}$ | (i) The free play nonlinearity reduces the cut-in wind speed and increased the output power.<br>(ii) Theoretically determining that the hardening stiffness brings the response amplitude to acceptable levels and broadens the operational wind speed range. |
| Bibo and Daqaq [68] | Piezoelectric | Modal convergence flutter | Airfoil, profile NACA0012 | 2.3 | — | 0.138*1 | 3 (With base acceleration 0.15 m/s$^2$) | Airfoil: semichord 4.2 cm, span 5.2 cm. Cantilever: — | $8.38 \times 10^{-4}$ | (i) Concurrent flow and base excitations enhances power generation performance.<br>(ii) Concurrent excitations increases output power by 2.5 times below the flutter speed, and over 3 times above the flutter speed.<br>(iii) Above the flutter speed, requiring careful adjustment because power is sensitive to base acceleration frequency. |
| Kwon [69] | Piezoelectric | Modal convergence flutter | Flat plate tip; Whole device T-shape | 4 | — | 4.0 | 15 | Flat plate tip: 6.0 × 3.0 cm$^2$. Cantilever: 10.0 × 6.0 × 0.02 cm$^3$ | 2.56 | (i) Simple T-shape structure, easy to fabricate.<br>(ii) No rotating components.<br>(iii) Wide operational wind speed range. |

Liya Zhao and Yaowen Yang. Toward Small-Scale Wind Energy Harvesting: Design, Enhancement, Performance Comparison, and Applicability. Shock and Vibration Volume 2017, Article ID 3585972, 31 pages, https://doi.org/10.1155/2017/3585972.

# Energy Harvesters Based on Wake Galloping

**Concept**

- Wake interactions from upstream bluff bodies cause oscillations in downstream structures.
- These oscillations are then converted into electrical energy, providing a new method for renewable energy harvesting.
- Passive energy harvesting using induced aerodynamic forces.

**Advantages**

- Can be designed to operate at varied wind directions.
- Potentially scalable for large-scale energy generation.

**Disadvantages**

- Complex fluid dynamics, requires careful placement of structures.

Liya Zhao and Yaowen Yang. Toward Small-Scale Wind Energy Harvesting: Design, Enhancement, Performance Comparison, and Applicability. Shock and Vibration Volume 2017, Article ID 3585972, 31 pages, https://doi.org/10.1155/2017/3585972.

# Energy Harvesters Based on Wake Galloping

| Author | Transduction | Prism shape | Cut-in wind speed (m/s) | Cut-out wind speed (m/s) | Maximum power (mW) | Wind speed at max power (m/s) | Dimensions | Power density per volume ($mW/cm^3$) | Advantages/disadvantages and other information |
|---|---|---|---|---|---|---|---|---|---|
| Jung and Lee [27] | Electromagnetic | Circular cylinder | ≈1.2 | — | 370.4 | 4.5 | Two identical cylinders: 5 cm in dia., 85 cm in length. Spacing distance: $5 \times D = 25$ cm. | 0.111 | (i) Determining the proper distance between the parallel cylinders for wake galloping energy harvesting, as 4-5 times the cylinder diameter, that is, $L/D = 4{\sim}5$. (ii) High output power. (iii) Wide operational wind speed range. (iv) Device volume is too big. |
| Abdelkefi et al. [74] | Piezoelectric | Windward: circular cylinder. Leeward: square cylinder | 0.4 | — | 0.04~0.05 | 3.05 | Circular cylinder: 1.25 cm in dia., 27.15 cm in length. Square cylinder: $1.28 \times 1.28 \times 26.67\ cm^3$. Spacing distance: 24 cm. Piezoelectric two identical cantilevers: $15.24 \times 1.8 \times 0.0305\ cm^3$. | $5.72 \times 10^{-4}$ | (i) Power from a galloping square cylinder was greatly enhanced by wake effects of an upstream circular cylinder. (ii) Operational wind speed range was widened by wake galloping. (iii) Diameter of the upstream cylinder and the spacing distance between two cylinders require careful adjustment. |

Liya Zhao and Yaowen Yang. Toward Small-Scale Wind Energy Harvesting: Design, Enhancement, Performance Comparison, and Applicability. Shock and Vibration Volume 2017, Article ID 3585972, 31 pages, https://doi.org/10.1155/2017/3585972.

# Energy Harvesters Based on Turbulence-Induced Vibration

**Concept**

- Random turbulence fluctuations cause small structural oscillations.
- Harvesting through piezoelectric/electromagnetic mechanisms.

**Applications**

- Urban wind energy harvesting

**Advantages**

- Highly applicable in turbulent environments.
- Low starting speed.

**Disadvantages**

- Requires robust design to withstand fluctuating loads.

Liya Zhao and Yaowen Yang. Toward Small-Scale Wind Energy Harvesting: Design, Enhancement, Performance Comparison, and Applicability. Shock and Vibration Volume 2017, Article ID 3585972, 31 pages, https://doi.org/10.1155/2017/3585972.

# Energy Harvesters Based on Turbulence-Induced Vibration

| Author | Transduction | Cut-in wind speed (m/s) | Cut-out wind speed (m/s) | Maximum power (mW) | Wind speed at max power (m/s) | Dimensions | Power density per volume ($mW/cm^3$) | Advantages/disadvantages and other information |
|---|---|---|---|---|---|---|---|---|
| Akaydin et al. [47] | Piezoelectric | $\approx 5^{*1}$ | — | $0.55 \times 10^{-4}$ | 11 | Bluff body: 3 cm in dia., 1.2 m in length. Cantilever: $3 \times 1.6 \times 0.02\ cm^3$. Distance from the wall: 4 cm | $6.48 \times 10^{-8}$ | (i) Performance of harvester in turbulent boundary layer depends on the distance from the wall; dominant oscillation frequency was close to the beam resonance frequency. |
| Hobeck and Inman [28] | Piezoelectric | $9 \sim 10^{*2}$ | — | 4.0 | 11.5 | Bluff body: $4.45 \times 4.45 \times 10.92\ cm^3$. Four identical cantilevers in an array: 101.60 mm × 25.40 mm × 101.60 $\mu$m steel substrate attached with 45.97 mm × 20.57 mm × 152.40 $\mu$m PZT | 0.0184 | (i) The first TIV energy harvesting model with experimental validation. (ii) Being robust and survivable due to its inherent redundancy, with minor reduction in total power caused by one damaged element. (iii) Suitable for highly turbulent fluid flow environments like streams or ventilation systems. |

Liya Zhao and Yaowen Yang. Toward Small-Scale Wind Energy Harvesting: Design, Enhancement, Performance Comparison, and Applicability. Shock and Vibration Volume 2017, Article ID 3585972, 31 pages, https://doi.org/10.1155/2017/3585972.

# Other Small-Scale Wind Energy Harvester Designs

- Damped cantilever pipe carrying flowing fluid
- Harmonica-type aeroelastic micropower generator
- Tensioned piezoelectric film facing laminar and/or turbulent incoming flows
- A hinged-hinged piezoelectric beam facing turbulent airflows
- A micromachined piezo electric airflow energy harvester inside a Helmholtz resonator

Liya Zhao and Yaowen Yang. Toward Small-Scale Wind Energy Harvesting: Design, Enhancement, Performance Comparison, and Applicability. Shock and Vibration Volume 2017, Article ID 3585972, 31 pages, https://doi.org/10.1155/2017/3585972.

# Other Small-Scale Wind Energy Harvester Designs

| Author | Transduction | Cut-in wind speed (m/s) | Cut-out wind speed (m/s) | Maximum power (mW) | Wind speed at max power (m/s) | Dimensions | Power density per volume ($mW/cm^3$) | Advantages/disadvantages and other information |
|---|---|---|---|---|---|---|---|---|
| Bibo et al. [75] | Piezoelectric | ≈5.5[*1] | — | 0.05 | 7.5 | Cantilever: $5.8 \times 1.626 \times 0.038\ cm^3$. Chamber volume: $2300\ cm^3$ | $2.17 \times 10^{-5}$ | (i) Mimicking the basic physics of music-playing harmonicas. (ii) Using optimal chamber volume and decreasing aperture's width reduce the cut-in wind speed. |
| Ovejas and Cuadras [76] | Piezoelectric | — | — | 0.0002 | 12.3 | Two identical bluff bodies: 0.5 cm in dia. Piezoelectric film: 15.6 cm × 1.9 cm × 40 $\mu$m | $1.25 \times 10^{-5}$ | (i) Bluff body configuration outperformed the one fixed side and two fixed side configurations. (ii) Rotational turbulent flow from a dryer added to vortex shedding effects, giving higher electrical output than the laminar flow did. |

Liya Zhao and Yaowen Yang. Toward Small-Scale Wind Energy Harvesting: Design, Enhancement, Performance Comparison, and Applicability. Shock and Vibration Volume 2017, Article ID 3585972, 31 pages, https://doi.org/10.1155/2017/3585972.

# Overview of Hydropower Plant

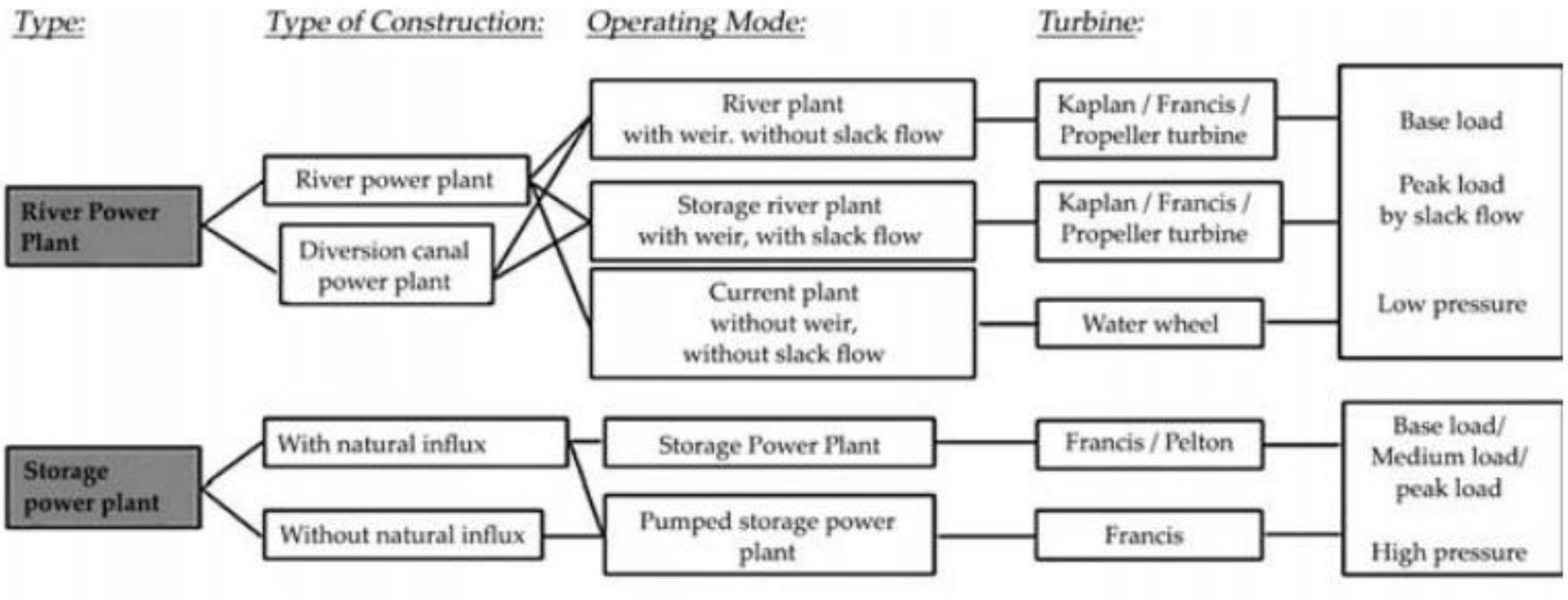


Source: https://link.springer.com/chapter/10.1007/978–3-642–20709–9_1.

# Hydroelectric Power Plant Component

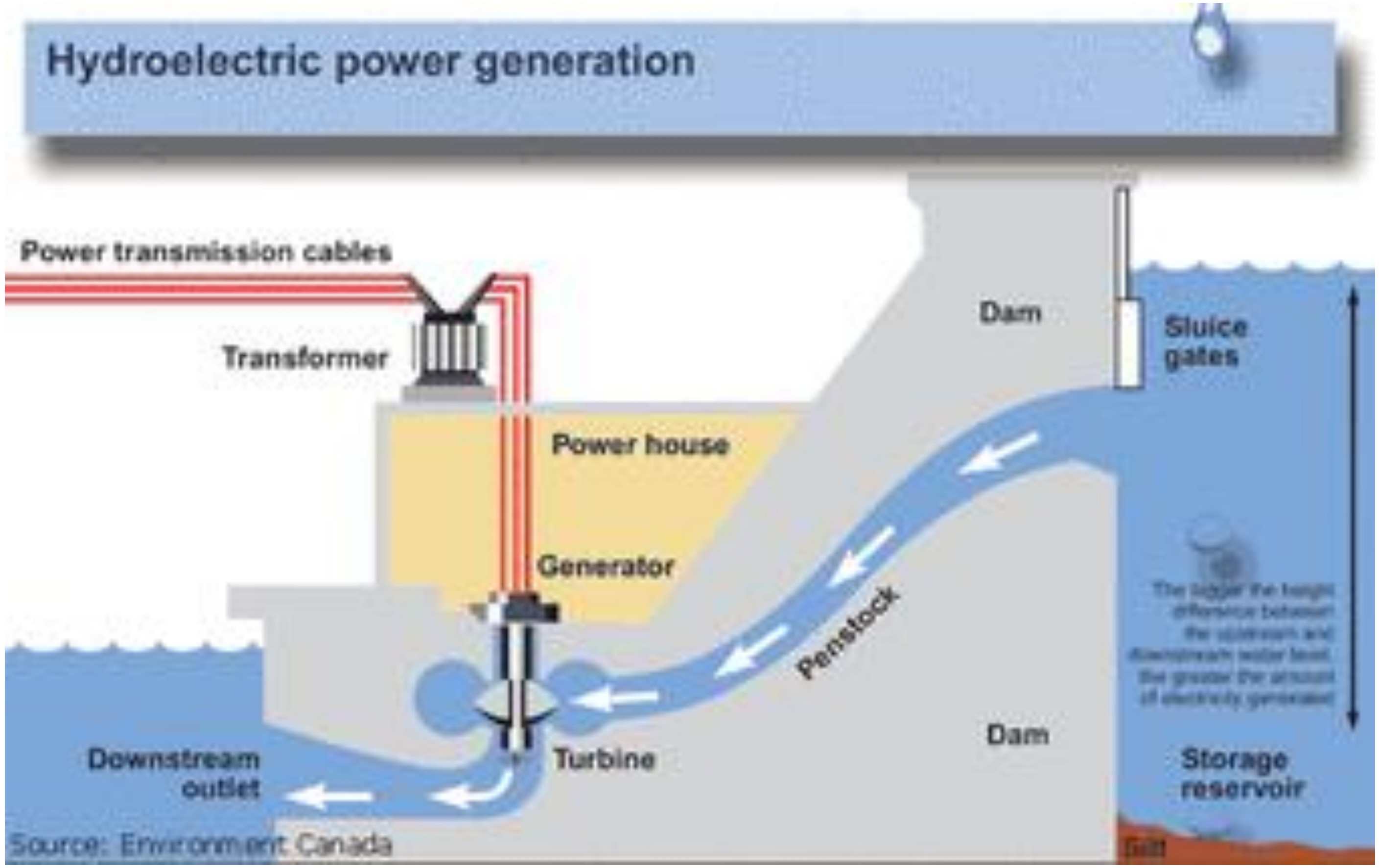


- **Forebay**: A reservoir or canal from which water is taken to run equipment (such as a waterwheel or turbine).
- **Penstock**: A closed conduit or pipe for conducting water to the powerhouse.
- **Power house**: The structure that houses generators and turbines.
- **Tailrace**: A channel that carries water away from a hydroelectric plant or water wheel.
- **Spillway**: A structure used to provide the release of flows from a dam into a downstream area.

https://www.usgs.gov/special-topic/water-science-school/science/hydroelectric-power-how-it-works?qt-science_center_objects=0#qt-science_center_objects

# Classification of Hydropower

- Classification by **Head and Size:**
- Classification according to size has led to concepts such as 'small hydro' and 'large hydro'
- Nevertheless, there is no worldwide consensus on definitions regarding size categories.
- Indonesia:

*Classification of hydro-power size (ref. 2)*

| Type | Capacity |
|---|---|
| Large hydro power | > 100 MW |
| Medium hydro power | 10 – 100 MW |
| Mini hydro power | 1 MW – 10 MW |
| Micro hydro power | 5 - 1000 kW |
| Pico hydro power | < 5 kW |

Source: DEN, 2017

Some countries defined small hydropower project such this:

**Table 5.3** | Small-scale hydropower by installed capacity (MW) as defined by various countries.

| Country | Small-scale hydro as defined by installed capacity (MW) | Reference Declaration |
|---|---|---|
| Brazil | ≤30 | Brazil Government Law No. 9648, of May 27, 1998 |
| Canada | <50 | Natural Resources Canada, 2009: canmetenergy-canmetenergie.nrcan-rncan.gc.ca/eng/renewables/small_hydropower.html |
| China | ≤50 | Jinghe (2005); Wang (2010) |
| EU Linking Directive | ≤20 | EU Linking directive, Directive 2004/101/EC, article 11a, (6) |
| India | ≤25 | Ministry of New and Renewable Energy, 2010: www.mnre.gov.in/ |
| Norway | ≤10 | Norwegian Ministry of Petroleum and Energy. Facts 2008. Energy and Water Resources in Norway; p.27 |
| Sweden | ≤1.5 | European Small Hydro Association, 2010: www.esha.be/index.php?id=13 |
| USA | 5–100 | US National Hydropower Association. 2010 Report of State Renewable Portfolio Standard Programs (US RPS) |

Source: IPCC, 2017

# Classification of Hydropower

Classification **by facility**:

1. Run-off River
2. Hydro storage / Dam
3. Pumped hydro Storage

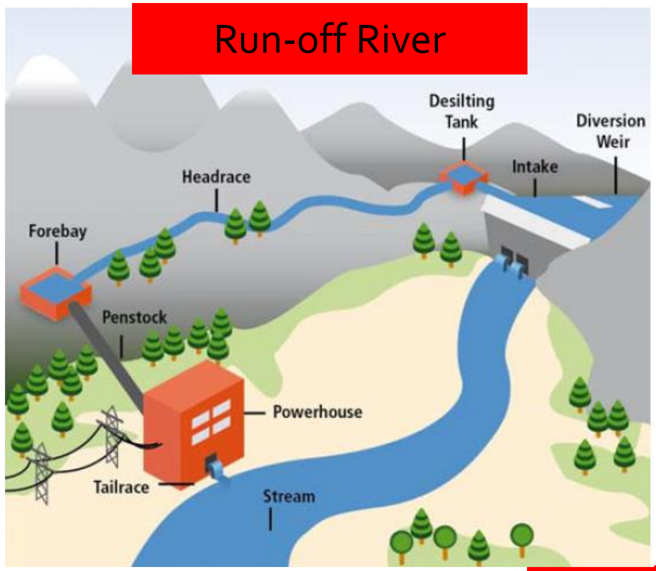


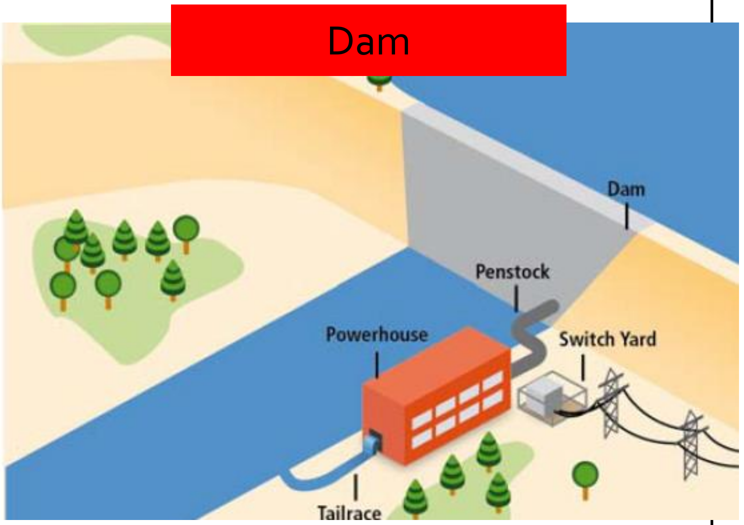


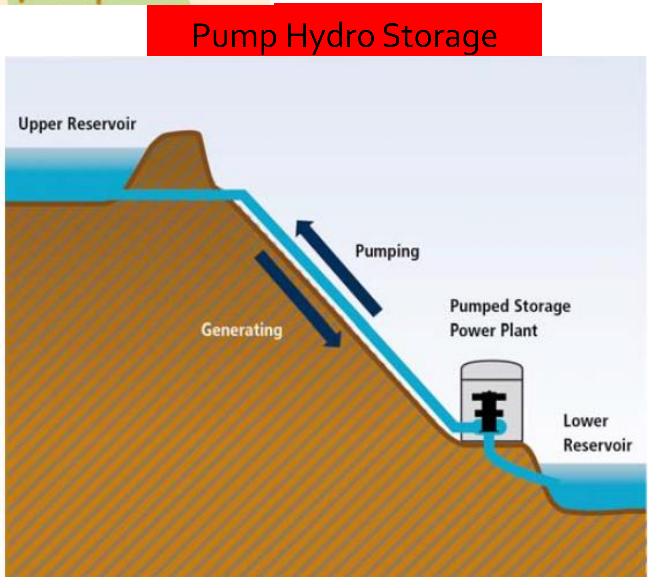


Source: IPCC, 2017

# Turbine

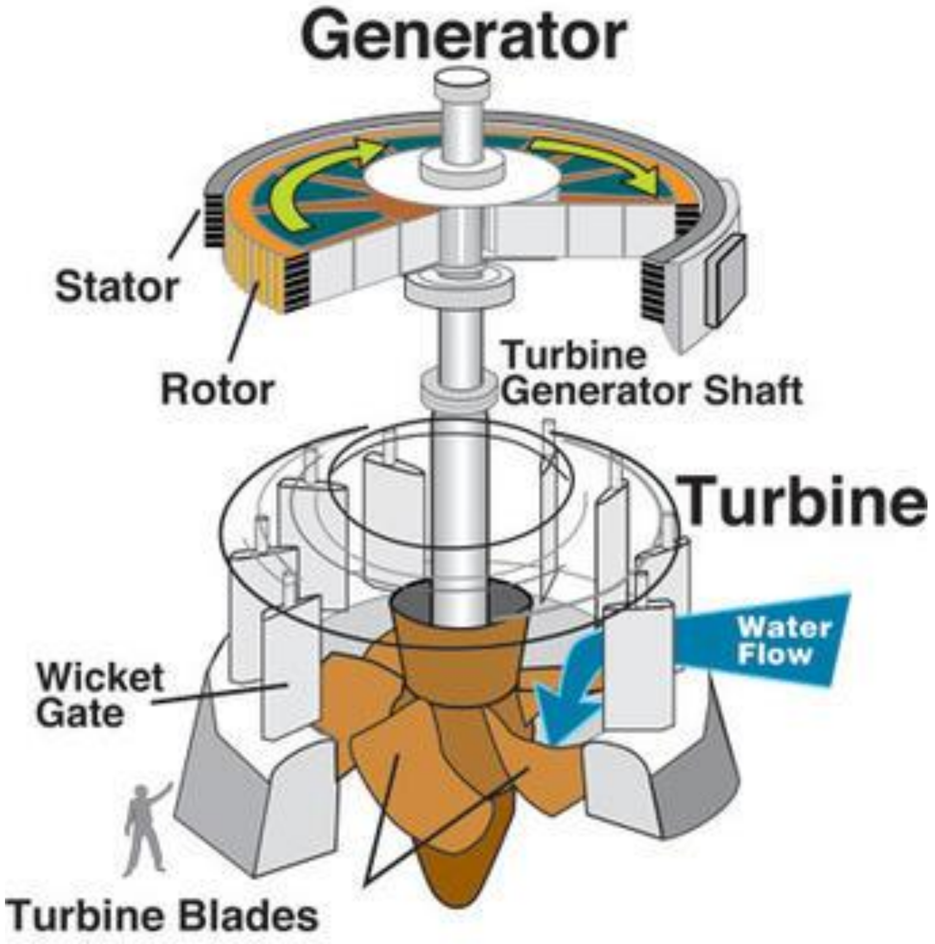


"The rotor is attached to the turbine shaft, and rotates at a fixed speed. When the rotor turns, it causes the field poles (the electromagnets) to move past the conductors mounted in the stator."

https://www.usgs.gov/special-topic/water-science-school/science/hydroelectric-power-how-it-works?qt-science_center_objects=0#qt-science_center_objects

# Hydraulic Power

$$P(\text{kW}) = \frac{e\ \gamma\ (\text{lb/ft}^3)\ Q\ (\text{ft}^3/\text{s})\ H_n\ (\text{ft})}{737}$$

$$P(\text{kW}) = \frac{e\ \gamma\ (\text{N/m}^3)\ Q\ (\text{m}^3/\text{s})\ H_n\ (\text{m})}{1000}$$

where $P$ = generator power output, kW
$e$ = turbine or generator efficiency as a fraction
$\gamma$ = specific weight of the water $\rightarrow \rho \cdot g$
$Q$ = turbine discharge
$H_n$ = net head on the turbine or generator unit

# Ballistic electrostatic generator

- A device that converts the inertial energy of jet drops into electric current.
- A jet of water is formed at the outlet of a pore of about thirty micrometers in diameter under the action of a strong over-pressure of the order of 100 kPa. The jet breaks into small drops. These drops possess an electrical charge which is induced by the surface charge of the hole.
- The charged drops arrive on the target plate which is connected to the ground. In this device, the acceleration of the drops compensates the electric field created between the bottom plate and the electrode.
- A current of electrons from the ground to the target plate is established. This current is counterbalanced by a current of electrons from the membrane to the ground.

Nan Wu, Youcef Brahmi and Annie Colin. Fluidics for energy harvesting: from nano to milli scales. Lab Chip,2023,23,1034

# Ballistic electrostatic generator

- Past study showed a conversion efficiency up to 48% and may generate a power density of 160 kW m−2 if scale up holds. However, the device is not yet developed as an application.

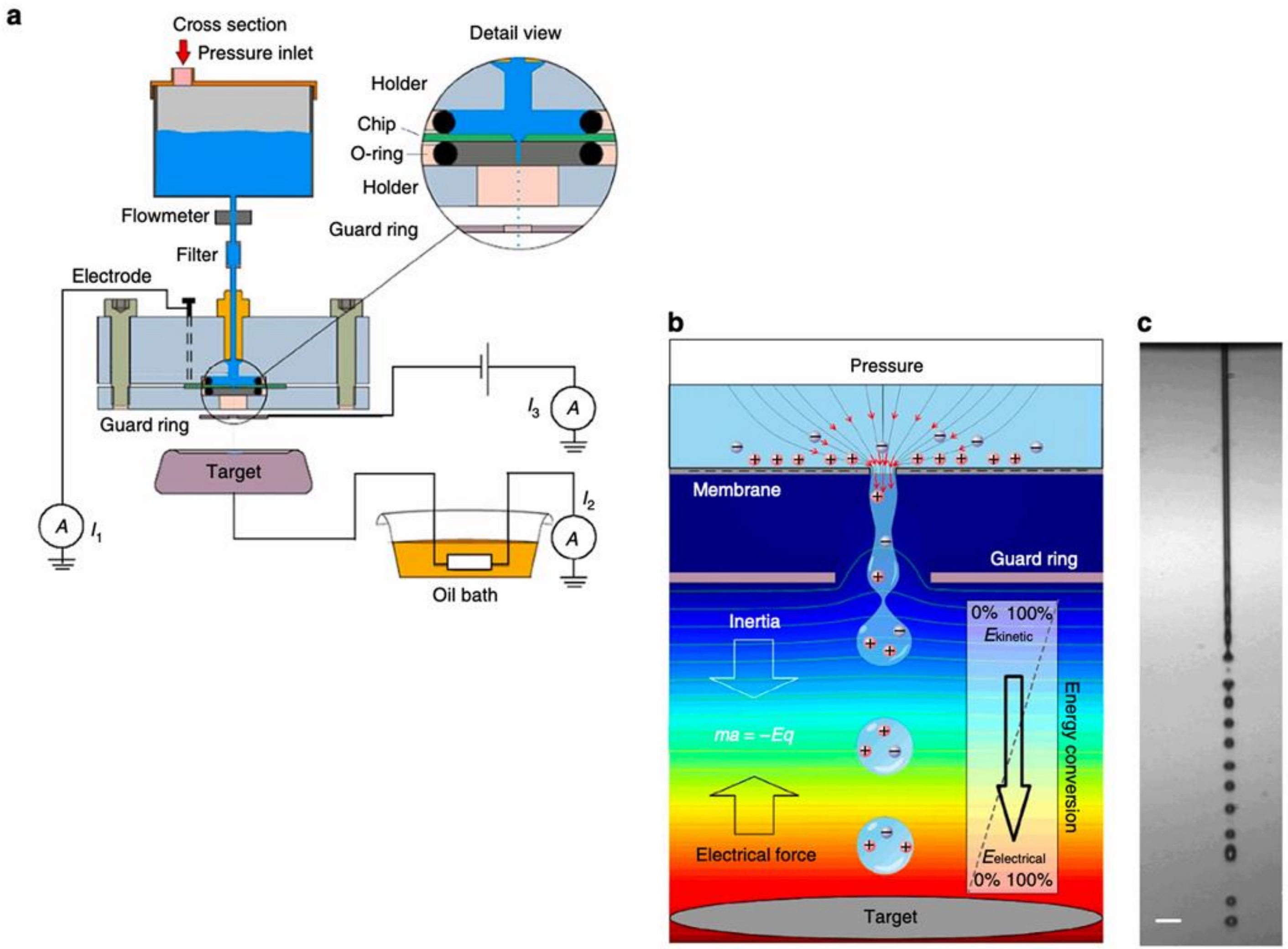


Nan Wu, Youcef Brahmi and Annie Colin. Fluidics for energy harvesting: from nano to milli scales. Lab Chip,2023,23,1034

# Harvesting energy of waves

- The triboelectric effect, which is also called triboelectricity, triboelectric charging, triboelectrification, or tribocharging, is when two objects slide or touch each other and an electric charge is transferred between them. It can happen between two pieces of the same material or between two pieces of different materials.
- Tribocharging has been seen to happen between solids, liquids, and gases
- Liquid–solid triboelectric technology is used to collect the energy of waves.
- A device involving the electrification of a liquid–solid contact was developed to recover wave energy. The material used is a film consisting of polytetrafluoroethylene (PTFE) nanoparticles. The PTFE is hydrophobic.

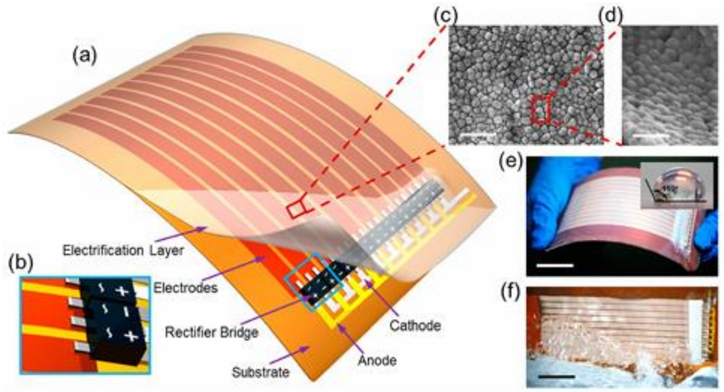


**Fig. 7** Structure of a thin-film triboelectric generator (TF-TEG). a, Schematic diagram of an integrated TF-TEG. b, Enlarged sketch of the arrayed bridge rectifiers. c, SEM image of the PTFE nanoparticles on the electrification layer (scale bar = 1 μm). d, Enlarged view of the nanoparticles at a tilted angle of 60° (scale bar = 500 nm). e, Picture of a bendable as-fabricated TF-TEG. Inset: Water contact angle on the nanostructured surface (scale bar = 25 mm). f, Picture of the TF-TEG that is interacting with the water wave (scale bar = 25 mm) (figures and captions reproduced from ref. 33 with permission from American Chemical Society, copyright 2015).

Nan Wu, Youcef Brahmi and Annie Colin. Fluidics for energy harvesting: from nano to milli scales. Lab Chip,2023,23,1034

# Harvesting energy of waves

- When the water comes into contact with the PTFE, the PTFE acquires a permanent electrostatic surface charge.
- During the following phases when the water advances on the surface, the positive ions it contains are adsorbed on the PTFE due to the existence of negative surface charge.
- As seawater propagates over the surface, this creates a charge gradient on the material, with the emerged part having zero charge and the dry part carrying an unbalanced negative charge.
- Electrons move away from electrode A whose surface charge is neutralized by the propagating water and head towards electrodes B and C which are both negatively charged.

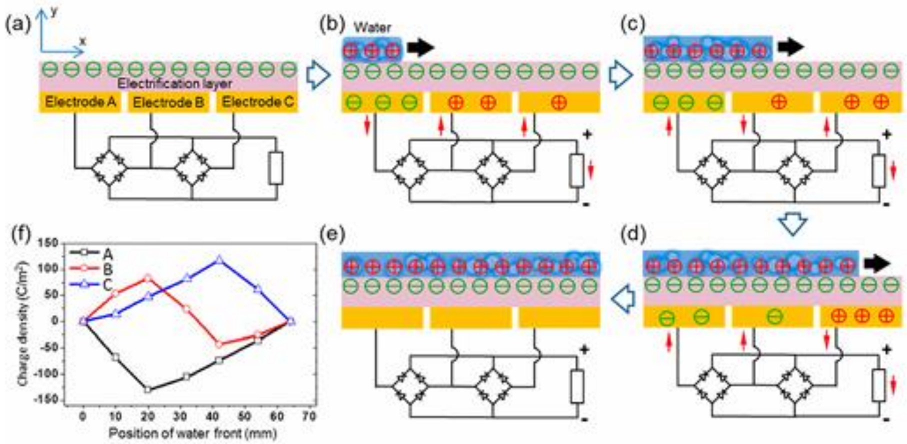


**Fig. 8** Electricity-generating process of the TF-TEG. (a) Cross-sectional view of charge distribution when the device is fully exposed from water. Charge distribution when water is propagating across (b) electrode A, (c) electrode B and (d) electrode C. (e) Charge distribution when water fully covers the electrification layer underneath. (f) Charge density on the three electrodes as the water front propagates (figures and captions reproduced from ref. 33 with permission from American Chemical Society, copyright 2015).

Nan Wu, Youcef Brahmi and Annie Colin. Fluidics for energy harvesting: from nano to milli scales. Lab Chip,2023,23,1034

# Hybridized triboelectric nanogenerator: coupling charge separation TENG and contact TENG

- When a raindrop falls, it brings with it charges but it also brings with it mechanical energy that can produce a current if it causes contact between two solids with different triboelectric properties.
- A very first approach concerned the coupled recovery of the kinetic energy and the electrostatic energy of water. When a raindrop or water falls, it not only brings charges, but also possesses a large amount of mechanical energy which can be harvested if a liquid/solid contact with different triboelectric properties is designed.
- This lead to the creation of hybridized Triboelectric Nanogenerators (TENGs), where a coupled recovery of kinetic energy and electrostatic energy is realized in a single system.

Nan Wu, Youcef Brahmi and Annie Colin. Fluidics for energy harvesting: from nano to milli scales. Lab Chip,2023,23,1034

# Hybridized triboelectric nanogenerator: coupling charge separation TENG and contact TENG

- an impeller whose blades are composed of superhydrophobic polytetrafluoroethylene (PTFE) thin films with nanostructures. These PTFE blades are used to harvest the electrostatic energy of the flowing water. The water flowing over the blades turns the wheel and sets in rotation a triboelectric disc that collects the mechanical kinetic energy.
- At a water flow rate of 54mL s−1, the device involving electrostatic energy has an open circuit voltage of 72V, a short circuit current of 12.9μA, and a maximum power of 0.59Wm−2.

Nan Wu, Youcef Brahmi and Annie Colin. Fluidics for energy harvesting: from nano to milli scales. Lab Chip,2023,23,1034